DESIGN OF SWITCHED MULTIBAND FILTERS FOR IEEE 802.11a/b/g WLANs

DR.S.RAGHAVAN*, SION.P

*Dr.S.Raghavan, Senior Professor,
Department of Electronics and Communication Engineering,
National Institute of Technology, Trichy, TamilNadu-620015,
India.
E-mail: raghavan@nitt.edu Fax: +91 431 2500133

Abstract:— Switched Multiband Microstrip bandpass filters for *IEEE* 802.11a/b/g WLANs are presented. Cross coupled square open loop resonator type of filter is used as the basic design. These filters were selected since there was a tuning parameter available in the structure which changed the center frequency without change in performance. Two MEMS reconfigurable filter structures are proposed. Static simulations for each position of the MEMS switches were performed for S_{11} and S_{12} to observe the bandwidth and insertion loss of the filter. The simulations were performed on IE3D 10.06.

Index Terms:— WLAN, MEMS, ISM, UNII, Microstrip Filter**.**

1. Introduction

The escalating deployment of wireless networking technology as well as other wireless technologies in the same unlicensed spectrum is rapidly increasing the radio frequency interference for Wi-Fi (802.11) products, threatening the data throughput performance of wireless local area network (WLAN). At the same time, the market is demanding higher data throughput rates for new WLAN applications like multimedia audio and video, streaming media, voice over WLAN, and others that require quality of service (QoS) capabilities and low packet error rates. Modern microwave communication systems require, especially in satellite and mobile communications, high performance narrow-band band pass filters having low insertion loss and high selectivity together with linear phase or flat group delay in the pass band. According to the early work on filter synthesis, it has been known that when frequency selectivity and band pass loss are considered to be the important filtering properties, then the optimum filters are those exhibiting ripple in both pass band and stopband. Such a filter response can be realized using filter with cross couplings between nonadjacent resonators. These cross couplings give a number of alternative paths which a signal may take between the input and output ports. Depending on the phasing of the signals, the multipath effect may cause attenuation poles at finite frequencies or group delay flattening, or even both simultaneously. Usually, the cross coupled resonator filters are realized using waveguide cavities or dielectric resonator loaded cavities because of their low loss. However, in order to reduce size, weight and cost there has been growing interest in planar structures. One difficulty in realizing the cross coupled microwave filters in the planar structures is to identify and control the required electric and magnetic couplings for the nonadjacent resonators. Compared with the Microstrip dual mode filters the Microstrip square open loop resonator filters can have a small size. Compared with the dual-plane multicoupled line filters the Microstrip open-loop resonator filters are much simpler in structure; they require no grounding and coupling apertures. It would also seem that the coupled square open loop resonators are more flexible to construct a variety of cross-coupled planar filters which have the similar coupling configurations as those of waveguide cavity cross-coupled filters. For the waveguide cavity cross-coupled filters, the design method, which is based on deriving a coupling matrix from the transfer function and realizing the coupling matrix in terms of intercavity couplings, is widely used for its simplicity and accuracy. It is thus desirable to adopt this synthesis technique to design cross-coupled Microstrip square open-loop resonator filters. However, the application of such a design approach requires the knowledge of mutual couplings between coupled Microstrip square open-loop resonators. The coupled structures result from different orientations of a pair of identical square open-loop resonators which are separated by a spacing s and may or may not be subject to an offset d. It is obvious that any coupling in those coupling structures is that of the proximity coupling, whish is basically, through fringe fields. The nature and the extent of the fringe fields determine the nature and the strength of the coupling. Each of the open-loop resonators has the maximum electric field density at the side with an open gap, and the maximum magnetic field density at the opposite side. Because the fringe field exhibits an exponentially decaying character outside the region, the electric fringe field is stronger near the side having the maximum magnetic field distribution. It follows that the electric coupling can be obtained if the open sides of the two coupled resonators are proximity placed , while the magnetic coupling can be obtained if the sides with the maximum magnetic field of two coupled resonators are proximity placed. For the coupling structure , the electric and magnetic fringe fields at the coupled sides may have comparative distributions so that both the electric and magnetic couplings occur. In this case the coupling may be referred to as the mixed coupling. As a consequence of an increasing amount of in-band and adjacent band interference in the environment for WLAN equipment; the design of radios and digital filtering has become critical. The problem of ACI (Adjacent Channel Interference) and a need for improved RF receiver performance for Wi-Fi and WLAN technology in both the 2.4 GHz and 5 GHz unlicensed bands has come to the attention of manufacturers, system designers, integrators and the Federal Communication Commission (FCC). Radio design should be in such a way that the WLAN's adjacent channel rejection (ACR) is improved for better overall performance. The situation motivates the need for tight RF band pass filtering at the receiver front end. Modern microwave communication systems require high-performance narrow-band bandpass filters having low insertion loss and high selectivity. When the frequency selectivity and bandpass loss are considered to be the important filtering properties, then the optimum filters are those exhibiting ripple in both passband and stopband. Such a filter response can be realized using filters with cross couplings between nonadjacent resonators. So cross coupled square open loop resonators [1] are taken as the basic structure. Since more and more functions are being incorporated into hand-held devices the available chip area has to be filled with multifunctional blocks. This is the motivation for reconfigurable structures. Reconfigurability is very near to realization by the advent of RF MEMS in microwaves. In this paper two switched Multiband structures are proposed. The filter which operates at two bands in 5GHz (5.15 GHz - 5.25 GHz and 5.25 GHz - 5.35GHz.) is discussed in the first section and the other which operates at 2.4 GHz and 5 GHz of MEMS switches is not dealt with in this paper. Hardwired (5.15 GHz-5.25 GHz) is discussed in the second section. The design of switches for simulation. The simulation software used is IE3D 10.06 [2]. Agile frequency selectivity, with increased quality factors and miniaturization, are probably the most valuable potential improvements within a radiofrequency front-end that can originate from the integration of RF-MEMS devices [3]-[5]. Alternative approaches are being investigated by the research community, in order to exploit the diversied and still non-standard MEMS technology. Very high-Q MEMS resonators, for example, are geared towards replacing crystal oscillators or SAW filters within future wireless transceivers . On the other hand, low-loss highly tunable passive networks are also most desirable [6], for implementing reconfigurable amplifier impedance matching networks , filters or oscillator tank circuits . For frequency spans of several GHz, as required by future multistandard wireless applications, RF-MEMS [7] technologies must provide switching elements with low insertion loss and high isolation, preferably integrating on the same high resistivity substrate high-Q inductors and capacitors. In this paper, a recently developed RF-MEMS ohmic switch technology is exploited for the design and fabrication of a dual frequency LC-tank on high resistivity Silicon substrate [8]. The wireless market is growing rapidly. Being pushed by market demands, various wireless communication systems are emerging. Wireless local area networks (WLANs) have been introduced in ISM and UNII bands for indoor wireless access. IEEE 802.16a Wireless Metropolitan Area Networks (WMANs) standard [11] published on 1 April 2003 for urban area coverage wireless access as the "last mile" solution. IEEE 802.16a system addresses frequencies from 2 to 11 GHz, including licensed and un-licensed bands while the dominant bands [12] are licensed bands of 2.3 GHz (WCS), 2.5 to 2.7 GHz (MMDS), 3.5 to 3.7 GHz (ETSI), and unlicensed bands of 2.4 GHz (ISM) and 5.8 GHz (U-NII) where WLANs operates as well [13][14]. In order to increase flexibility on the market and functionality of RF transceivers, multi-band and/or multistandard transceiver architecture solutions are pursued. A straight forward method is to use multi-input stage for each interested frequency. The advantage of the approach is that the performances of each RF front-end can be optimized for each frequency band, but it suffers from area and cost issues. In this paper, a multi-band multi-standard receiver architecture with maximum hardware sharing for IEEE 802.16a and IEEE 802.11a/b/g is developed. A single wideband input matching LNA and a multi-band down conversion mixer are proposed and implemented to save the chip area and cost. the proposed multi-band multi-standard receiver for IEEE 802.11a/b/g and IEEE 802.16a. Dual conversion architecture is used for IEEE 802.11a/b/g and IEEE 802.16a. But zero-IF technique is adopted for 3.5~3.7GHz the IEEE 802.16a ETSI band. Since IEEE 802.11b/g, and WCS and MMDS bands of IEEE 802.16a share adjacent frequency bands around 2.4 GHz, the RF filter can be used for these standards. For this band, the first local oscillator (LO) frequency is located at 3.45 to 4.05 GHz to convert the signal to IF band from 1.15 to 1.35 GHz and then the second LO frequency converts it to the baseband. IEEE 802.11a and U-NII band of IEEE 802.16a also share the same frequency band so that the RF filter can be used for these two standards. For the U-NII band, the first LO frequency is placed at 3.85 to 4.37 GHz to convert the signal to 1.282 ~ 1.457 GHz and then the second LO transfers the signal to the baseband. For the ETSI band, the received signal is directly converted to baseband through the first LO. During recent years, the increasingly wider use of portable electronic devices has caused a real revolution in communications systems. In order to allow notebooks, personal data assistants (PDAs), and cellular telephones to share information and communicate anywhere, many protocols and standards for wireless systems have been defined. Nowadays, we can choose to access communication networks with different provided services, transmission rates, and coverage areas. The most widespread wireless systems are Bluetooth, IEEE 802.11a,b,g, and HIPERLAN; they all work in the 2.4-GHz free industrial scientific medical (ISM) band and in the 5-GHz frequency band. The increasing demand for interoperability in mobility has necessitated the design of Multiband compact radiating elements. Many studies and design solutions for Multiband and miniaturized antennas have been presented . The reduced availability of space in portable terminals imposes the design of high-performance elements with the characteristics of small size, lightness, and compatibility with all the electronic devices integrated in the terminal itself. Some techniques used to reduce size consist of cutting slots in the radiating metallic traces so to create additional paths for currents.

A dual band MEMS-CMOS RF oscillator prototype is also realized and tested, following a chip-on-chip and wire bonding integration of the separate CMOS die on the RF-MEMS substrate. The technology process utilized for the fabrication of the ohmic switches is based on surface micromachining, with an electroplated suspended gold membrane layer, one polysilicon layer for the actuation electrodes and a TiN-Ti-Al-TiN-Ti multi-layer for the RF-signal path. A detailed process description is given by the authors in [9] . A shunt and a series switch configurations are available, both achieving similar insertion loss and isolation. An inter digitized configuration for the actuation and signal electrodes is adopted, for improved contact pressure spreading across the switch area [15]-[20] . The shunt ohmic switch is included in the LC-tank network of the present work. A layout of a single ohmic shunt switch , with a descriptive cross-section of the suspended plate and underlying actuation and signal electrodes. Input and output RF ports are physically connected by the signal fingers underneath the gold membrane, leading to a close switch state when the suspended plate is in its up-state position.

For wide-area cellular systems, such as IS-95 Code-Division Multiple Access (CDMA) and the third generation (3G) Wide-band CDMA (W-CDMA), transmit power control (TPC) is critically important in order to (1) ameliorate the near-far problem, specifically, for CDMA uplink systems; (2) minimize the interference to/from other cells, i.e., co-channel interference; and (3) improve the system performance on fading channels by compensating fading dips [21]. For wireless local area networks (WLANs), which are mainly used in indoor home, office, and public access environments, TPC has not attracted enough attention as it was not considered as critical to success as in CDMA systems. However, since many WLAN devices such as laptops and palmtops are battery-powered, and extending the operation time of such devices is always desirable, applying TPC in WLAN systems in order to save the battery energy can be naturally an attractive idea. Moreover, in the multi-cell WLAN systems often found in office and public access environments, reducing the co-channel interference via TPC could be quite beneficial as well since it results in better error performance in a given area. In this paper, we demonstrate the energy-efficient data transmission in IEEE 802.11a WLANs by combining TPC with physical layer (PHY) rate adaptation. In recent years, several power-management policies have been proposed to force a WLAN device to sleep adaptively at appropriate moments to save battery energy. In [22], the authors used the Time-Indexed Semi-Markov Decision Process (TISMDP) model to derive the optimal policy for dynamic power management in portable systems. In [23]-[24], several application-specific policies were given to put an idle WLAN device into sleeping mode. However, both papers assumed a fixed transmit power level. Since TPC determines the best transmit power level to use in transmit mode, it is complementary to these power-management policies, which address how to switch between transmit/receive and sleeping modes [26]-[31].

2. Filter- I

2.1. Structure

The dimensioned filter structure is as shown in Fig.1.

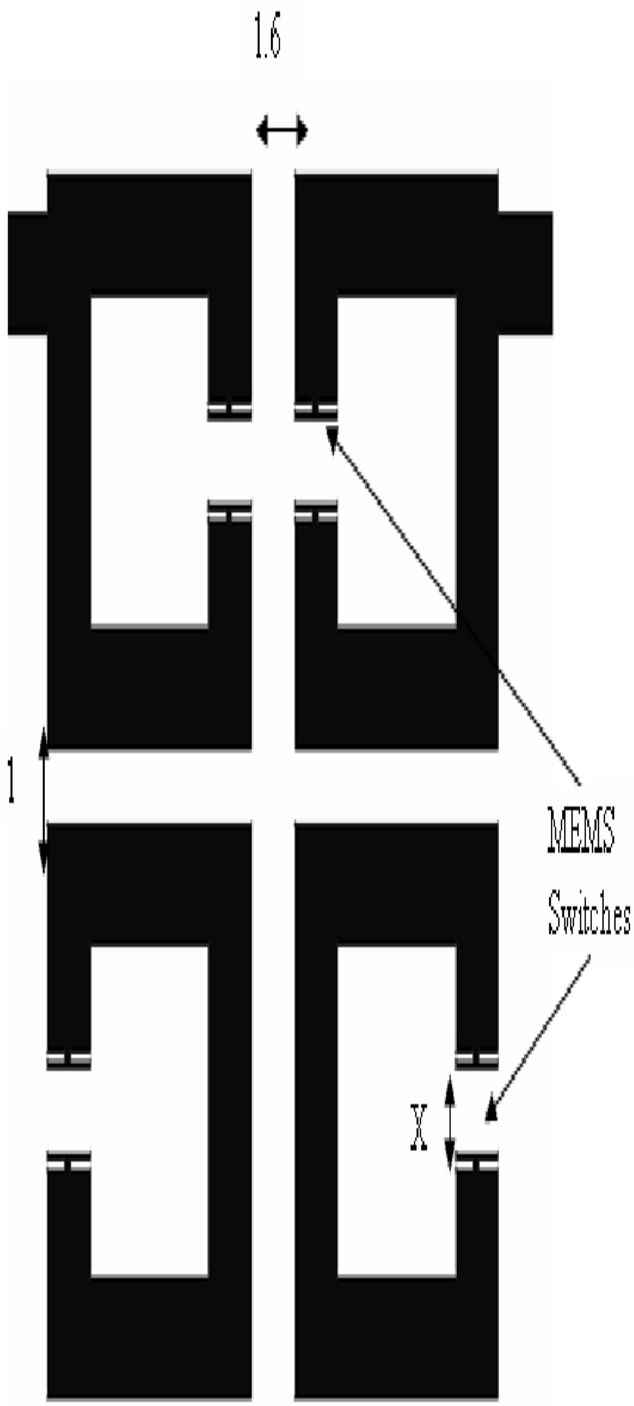

Fig. 1 Layout of the reconfigurable filter for two bands in 5GHz band

The substrate has a dielectric constant of e_r = 2.2 and thickness of h = 0.5mm. The overall size of the filter shown in Fig.1 is 16.055 mm X 15.655 mm (~0.23λo X 0.23 λo) where λo is the free space wavelength at 5.2 GHz. For the first band 5.15 GHz - 5.25 GHz the dimension 'X' is 1.08mm and for 5.25 GHz -5.35 GHz the dimension 'X' is 1.5 mm. The size of the resonator is 7.428 mm X 7.428 mm. Hardwired switches are used for static simulation of the structure at two different frequencies. When the switches are in the ON state the gap width will be 1.08 mm and the filter operates at 5.2 GHz center frequency whereas when the switches are in the OFF state the gap width will be 1.5 mm and the filter will be operating in the 5.3 GHz center frequency.

2.2. Results

The structure was simulated using IE3D electromagnetic simulation tool. The return loss and transmission loss of the structure as obtained from the simulation is shown in Fig.2.

Fig.2a shows the S_{12} response when the switches are in the ON state and OFF state. Similarly Fig.2b shows the S_{11} response in two states of the switches. The parameters of the filter obtained from simulation have been summarized in the Table I given below. The filter for the first band is having a passband extending from 5.148 GHz -5.245 GHz and that for the second band is having a passband extending from 5.24 GHz-5.34 GHz. The insertion losses have been increased by around .8dB than if it were simulated without hardwired switches.

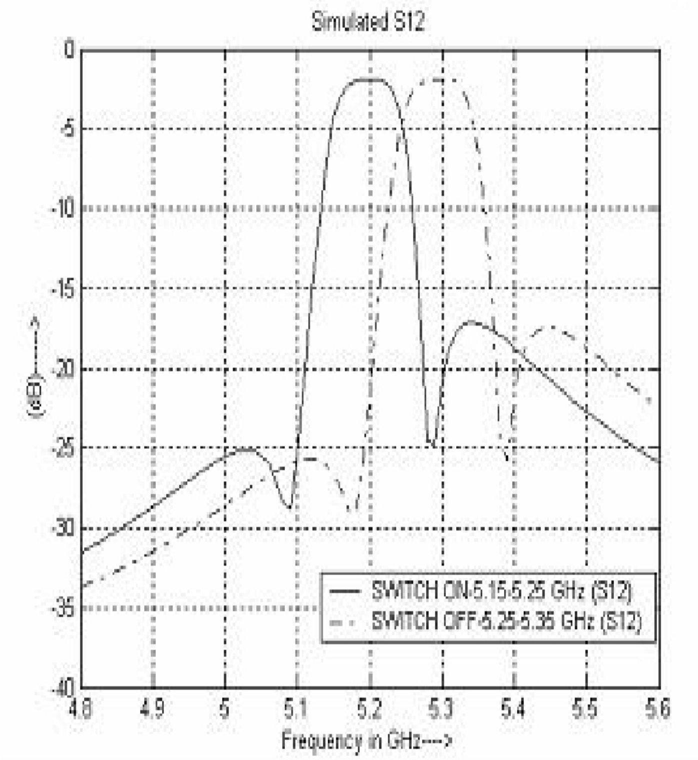

(a)

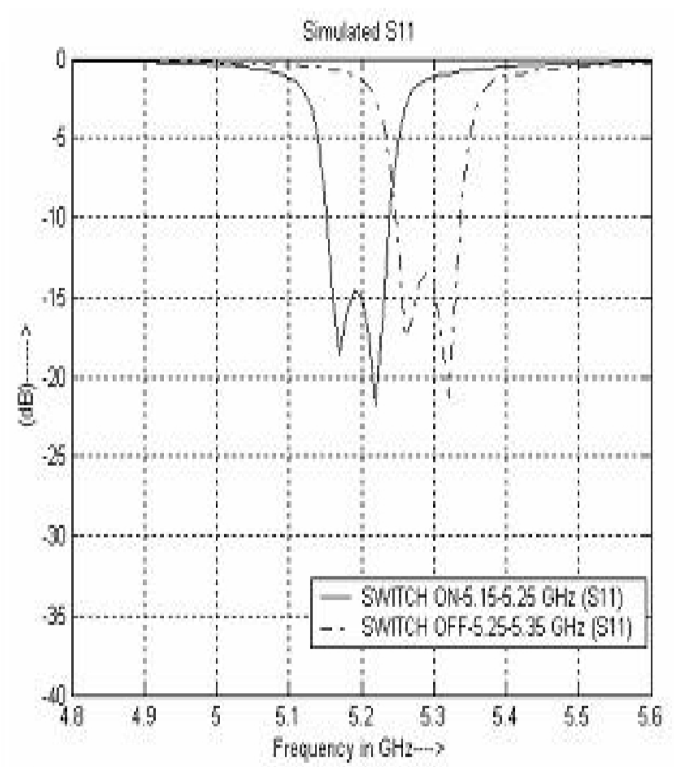

(b)

Fig.2. Response of the filter shown in Fig.1. a) S_{12} b) S_{11}

Table 1. Parameters of the filters in 5GHz band obtained through simulation

Switch State	Center Frequency (GHz)	3-dB Bandwidth (MHz)	Maximum Return Loss(dB)	Insertion Loss(dB)
Switch ON	5.2	96.3	>15	1.88
Switch OFF	5.31	100	>13.5	1.88

3. Filter - II

3.1. Structure

The filter for 2.4GHz band will come to about 27 mm x 27 mm and the filter for 5 GHz will have a size of 16 mm x 16 mm**.** This brings the idea of keeping the high frequency filter inside the low frequency one and providing switches so that the filter can operate in both bands with the size required for only one filter. The structure arrived at is a bit complex in that around 8 switches have to be operated for each state. The biasing lines have to be provided and open stubs also should be provided for all the switches. So the filter was designed to operate only in two bands (2.4 GHz and 5.15 GHz - 5.25 GHz). It can also be made to operate in 5.25 GHz - 5.35 GHz by taking up the design just discussed. But it will need 4 extra switches to be incorporated in the structure which will make the structure still complex. The structure is as shown in Fig.3. The substrate has a dielectric constant of ε_r = 2.2 and thickness of h = 0.5 mm. The overall size of the filter is 27.726 mm x 28.126 mm. All the small sized gaps shown in the figure are switches. For uniformity the gap width has been set as 0.3 mm. The filter shown (Fig 3a) is configured for operation at 2.4 GHz. Switching on the switches which are currently OFF (switch set B) and switching OFF the others (switch set A) and switching the ports will make the filter to work in the 5 GHz band (Fig.3b). The input for the inside filter can be given by a wire connection passing over the outside filter to a small line which can be placed outside the full layout.

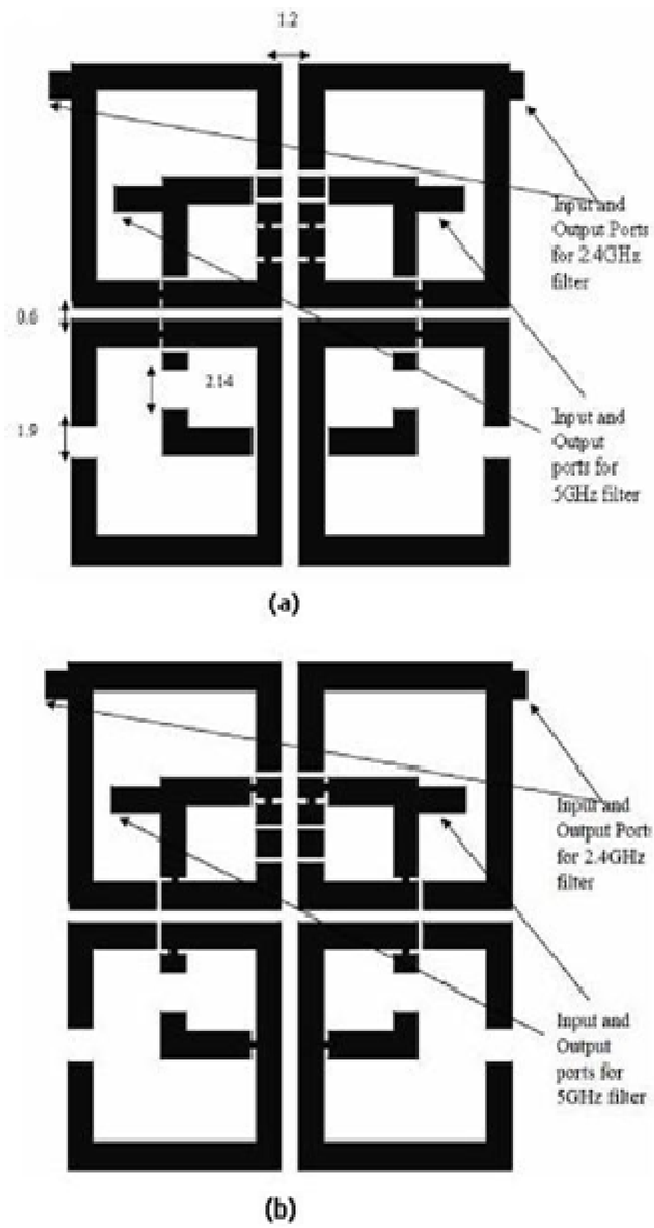

Fig.3. Layout of the reconfigurable filter operating at a) 2.4 GHz and b) 5 GHz.

3.2. Results

The return loss and transmission loss of the structure as obtained from the simulation is shown in Fig. 4. Fig. 4a shows the S_{21} plot of the structure in the two states of the switches and Fig.4b shows the S_{11} plot of the structure in the two states. Fig.4a shows a spurious response around 4.7 GHz which is a characteristic of this type of filter. But this is outside the 5 GHz band which is of present concern. Similarly the filter shows a spurious response at 2.8 GHz which is not supposed to come for this type of filters. This may be due to the effect of structure surrounding the 5 GHz filter. But this is also not affecting the 2.4 GHz band. The spurious responses can easily be removed by using one or two shunt stubs giving a notch at the desired frequency. Fig. 5 shows the plots of Fig. 4 in the corresponding areas of operation. The parameters of the filter obtained from simulation have been summarized in the Table 2 given below.

Table 2. Parameters of the filter in Fig. 5 obtained through simulation

Switch State	Center Frequency GHz)	3-dB Bandwidth (MHz)	Maximum Return Loss(dB)	Insertion Loss(dB)
Switch set A ON	2.44	77	>14	1.21
Switch set B ON	5.21	97.8	15	1.479

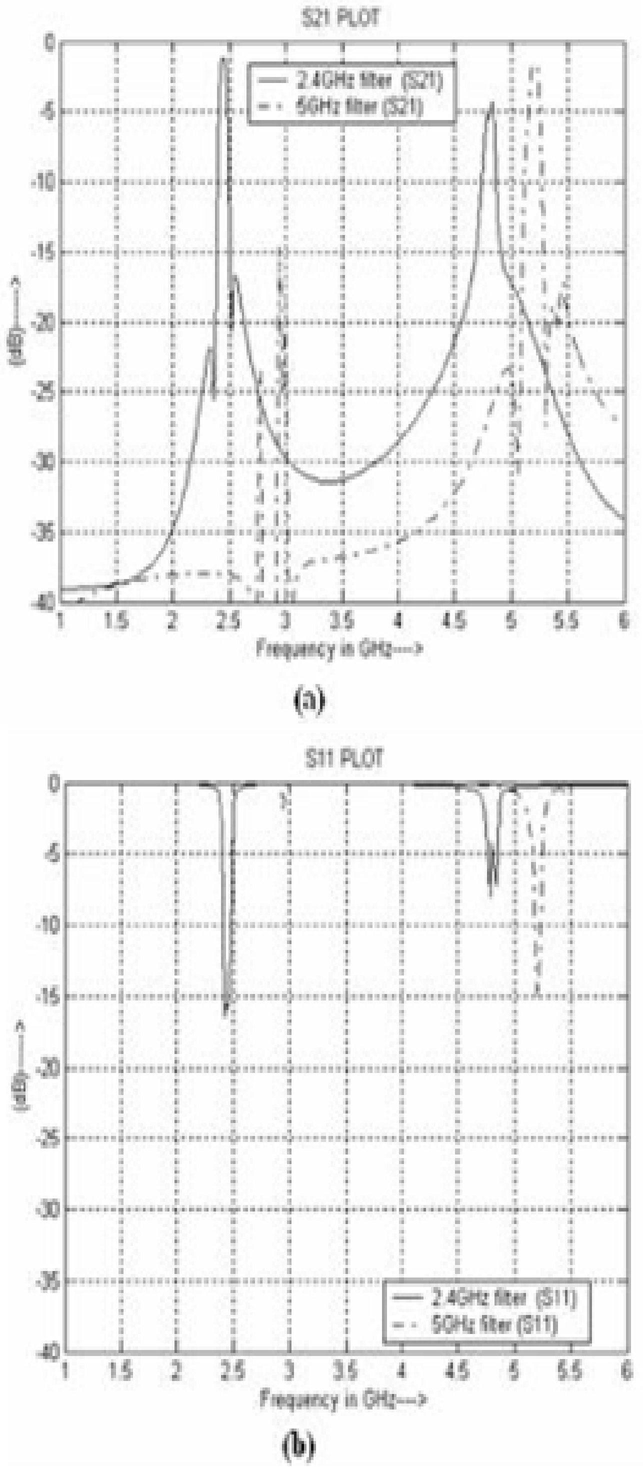

Fig. 4 Simulated response of the filter for two states of the switches a) S12 b) S11

The filter for the first band is having a passband extending from 2.407 GHz- 2.484 GHz and that for the second band extending from 5.154 GHz-5.252 GHz. The first filter configuration can get a bandwidth of 84 MHz (now 77 MHz) just by moving down 0.5 dB from the 3 dB point. The structure was simulated using IE3D electromagnetic simulation tool. The return loss and insertion loss of the structure as obtained from the simulation, which makes the filter to operate in 2.4 GHz band and the same when the other set of switches which were in the OFF state is turned ON and vice versa. This makes the filter to operate at 5.15 GHz – 5.25 GHz. Spurious response around 4.7 GHz which is a characteristic of this type of filter. But this is outside the 5 GHz band which is of present concern. Similarly spurious response at 2.8 GHz which is not supposed to come for this type of filters. This may due to the effect of structure surrounding the 5 GHz filter. But this is also not affecting the 2.4 GHz. The spurious can easily be removed by using one or two shunt stubs giving a notch at the desired frequency.

4. Conclusion

Implementation of bandpass filters for IEEE 802.11A/B/G WLAN's is presented in this paper. Two switched Multiband filter structures were proposed with the basic structure as cross coupled square open loop resonator. The first structure was designed for the first two bands in 5 GHz slot and the second structure was designed for 2.4 GHz and first band in 5 GHz slot. The results were acceptable for practical realization except for the stopband attenuation which should be improved further. The various designs presented highlights the possibility of reconfiguration in filters structures and thereby bringing out the feasibility of multiple system on a chip. Further reduction in size as well as stringent selectivity should be made possible in these designs since these are going to be a part of portable handheld devices working in congested traffic bands.

References:

[1] Jia Sheng Hong, M.J. Lancaster, *"*Couplings of Microstrip Square Open Loop Resonators for Cross Coupled Planar Microwave Filters*", IEEE Trans.* o*n Microwave Theory and Techniques, Vol.44, No.12, December 1996.*

[2] IE3D Version 10.06, *Users Manual, Zeland SoftwareInc.*

[3] Houle Gan, Dongwu Lou and Dongxia Yang, "Compact Microstrip Bandpass Filter with Sharp Transition Band", IEEE Microwave and Wireless Components Letters, Vol. 16, no.3, March 2006.

[4] S.Jovanovic and A.Nesic, "Microstrip Bandpass Filter with new Type of Capacitive Coupled Resonator", Electronics Letters, vol.41, no.1, January 2005.

[5] Cedric Quendo, Eric Rius, and Christian Person, "Narrow Bandpass Filters Using Dual-Behavior Resonators", IEEE Trans. On Microwave Theory and Techniques, vol.51, no.3, March 2003.

[6] Jia Sheng Hong, M.J.Lanscator, "Couplings of Microstrip square open loop Resonators for Cross Coupled Planner Microwave Filters", IEEE Trans. On Microwave Theory and Techniques, vol.44, no.12, December 1996.

[7] Gabriel M.Rebeiz, "RF MEMS Theory, Design and Technology", John Wiley and Sons, 2001.

[8] Yoonjae Choi, Byeongjik Lee, Jinsuk Pak, Icksoo Lee, Hoseseung Lee, Jangkyu Yoon, Kijun Han, "An Adaptive TXOP Allocation in IEEE 802.11e WLANs", WSEAS Transaction on Communications, vol.6, April 2007, pp. 518-523.

[9] M. K. Khan, R.A. Carrasco, I.J.Wassell, "Application of High Rate LDPC Codes for IEEE 802.16d or WiMax (Fixed Broadband) Systems, WSEAS Transaction on Communications, vol.6, Jan 2007, pp. 92-97.

[10] Padma Bonde, Jayesh Bonde, "HIPERLAN/2 and 802.11a: A Comparative Study", WSEAS Transaction on Communications, vol.5, March 2006, pp. 449-453.

[11] Ramjee Prasad and Tero Ojanpera, "An Overview of CDMA Evolution toward Wideband CDMA," *IEEE Communications Surveys*, vol. 1, no. 1, pp. 2–29, Fourth Quarter 1998.

[12] IEEE 802.11, *Part 11: Wireless LAN Medium Access Control (MAC) and Physical Layer (PHY) Specifications*, Standard, IEEE, Aug. 1999.

[13] IEEE 802.11a, *Part 11: Wireless LAN Medium Access Control (MAC) and Physical Layer (PHY) Specifications: High-speed Physical Layerin the 5 GHz Band*, Supplement to IEEE 802.11 Standard, Sep. 1999.

[14] Daji Qiao and Sunghyun Choi, "Goodput Enhancement of IEEE 802.11a Wireless LAN via Link Adaptation," in *Proc. IEEE ICC'01*, Helsinki, Finland, Jun. 2001.

[15] Steven D. Gray and Venkatesh Vadde, "Throughput and Loss Packet Performance of DCF with Variable Tranmit Power," IEEE 802.11-01/227, May 2001.

[16] Sunghyun Choi, "PCF vs. DCF: Limitations and Trends," IEEE 802.11- 01/154, Jan. 2001.

[17] IEEE 802.11h/D1.0, *Part 11: Wireless LAN Medium Access Control (MAC) and Physical Layer (PHY) Specifications: Spectrum and Transmit Power Management extensions in the 5 GHz band in Europe*, Draft Supplement to IEEE 802.11 Standard-1999 Edition, Draft 1.0, Jul 2001.

[18] Tajana Simunic, Luca Benini, Peter Glynn, and Giovanni De Micheli, "Dynamic Power Management for Portable Systems," in *Proc. ACM MobiCom'00*, Boston, MA, Aug. 2000, pp. 11–19.

[19] Mark Stemm, Paul Gauthier, Daishi Harada, and Randy H. Katz, "Reducing Power Consumption of Network Interfaces in Hand-Held Devices," in *Proc. 3rd International Workshop on Mobile Multimedia Communications*, Princeton, NJ, Sep. 1996.

[20] Paul Lettieri, Christina Fragouli, and Mani B. Srivastava, "Low Power Error Control for Wireless Links," in *Proc. ACM MobiCom'97*, Budapest, Hungary, 1997, pp. 139–150.

[21] J. G. Proakis, *Digital Communications, 3rd ed.*, McGraw Hill, New York, NY, 1995.

[22] M. B. Pursley and D. J. Taipale, "Error Probabilities for Spread-Spectrum Packet Radio with Convolutional Codes and Viterbi Decoding," *IEEE Transactions on Communications*, vol. COM-35, no. 1, pp. 1–12, Jan. 1987.

[23] D. Haccoun and G. Begin, "High-Rate Punctured Convolutional Codes for Viterbi and Sequential Decoding," *IEEE Transactions on Communications*, vol. 37, no. 11, pp. 1113–1125, Nov. 1989.

[24] Agere Systems, *User's Guide for ORiNOCO PC Card*, Sep. 2000.

[25] Intersil Americas Inc., *Prism II 11Mbps Wireless Local Area Network PC Card*, Apr. 2001.

[26] Intersil Americas Inc., *2.4 GHz Power Amplifier and Detector*, Mar. 2000.

[27] IEEE 802.11b, *Part 11: Wireless LAN Medium Access Control (MAC) and Physical Layer (PHY) Specifications: High-speed Physical LayerExtension in the 2.4 GHz Band*, Supplement to IEEE 802.11 Standard, Sep. 1999.

[28] John F. Sevic, "Statistical Characterization of RF Power Amplifier Efficiency for CDMAWireless Communication Systems," in *Proc.Wireless Communications Coonference*, Boulder, CO, Aug. 1997, pp. 110–113.

[29] M. Rofougaran, A. Rofougaran, C. Olgaard, and A. A. Abidi, "A 900 MHz CMOS RF Power Amplifier with Programmable Output," in *1994 Symposium on VLSI Circuits Digest of Technical Papers*, Jun. 1994, pp. 133–134.

[30] Bob O'Hara and Al Petrick, *The IEEE 802.11 Handbook: A Designer'sCompanion*, Standards Information Network, IEEE Press, 1999.

[31] S. Choi, S. Gray, M. Kasslin, S. Mangold, A. Soomro, A. Myles, D. Skellern, and P. Ecclesine, "Transmitter Power Control (TPC) and Dynamic Frequency Selection (DFS) Joint Proposal for 802.11h WLAN," IEEE 802.11-01/169r2, May 2001.